ISAS - INTERNATIONAL SCHOOL FOR ADVANCED STUDIES

Parametrization of Shadow Wave Function for Non-Homogeneous Quantum Systems

Thesis submitted for the degree of Magister Philosophiae

Condensed Matter Sector

Candidate:
Francesco Pederiva

Supervisor:
Prof. Stefano Fantoni

November 1992

TRIESTE

SISSA - SCUOLA INTERNAZIONALE SUPERIORE STUDI AVANZATI
TRIESTE
Strada Costiera 11

Parametrization of Shadow Wave Function for Non-Homogeneous Quantum Systems

Thesis submitted for the degree of
Magister Philosophiae

Condensed Matter Sector

Candidate:
Francesco Pederiva

Supervisor:
Prof. Stefano Fantoni

November 1992

Contents

1

Introduction

Microscopic calculations on quantum liquids and solids have been extensively performed in the last few years. Among these systems ^{4}He is one of the most studied and most of its properties have been basically understood. The HFDHE2 Aziz pseudopotential [1] has been found to describe realistically the He-He interaction particularly in the liquid phase, where it reproduces the experimental saturation density $\rho = 0.365$ and the binding energy per particle $E = -7.14K$ [2]. However, many problems remain still to be solved, expecially from the quantitative point of view. Simulation techniques have been found to be very useful to study ^{4}He. In particular it has been possible to solve exactly the Green Function Monte Carlo (GFMC) for the ground state of liquid ^{4}He.

Variational calculations. The Variational Monte Carlo method consists in calculating the expectation value of operators on a given trial wave function using the Metropolis algorithm. (See for example ref. [2] The expectation value of the Hamiltonian H verifies the inequality:

$$E_{GS}^{var} = \frac{\int dR \Psi_T(R) H \Psi_T(R)}{\int dR \Psi_T^2(R)} \geq E_0 \tag{1.1}$$

where E_0 is the ground state energy. If we define the *local energy*

$$E_L = \frac{H\Psi_T(R)^2}{\Psi_T(R)} \tag{1.2}$$

the calculation of E_{GS}^{var} corresponds to estimating $\langle E_L \rangle_P$ where the probability distribution P is defined as

$$\frac{\Psi_T(R)}{\int dR \Psi_T^2(R)} \tag{1.3}$$

and is sampled by standard Metropolis algorithm.

The hamiltonian of N ^{4}He atoms is given by:

$$H = T + \sum_{i<j} v(r_{ij}) \tag{1.4}$$

where the two body potential has strong repulsion at short interatomic distances, which induce strong He-He correlations. We can write the ground state for H as the product of two functions:

$$\psi_0(\vec{r}_1 \cdots \vec{r}_N) = F(\vec{r}_1 \cdots \vec{r}_N)\phi(\vec{r}_1 \cdots \vec{r}_N) \tag{1.5}$$

where ϕ is a mean field wave function with the proper behaviour under exchange of particles (symmetric for bosons and antisymmetric for fermions).If we restrict ourselves to homogeneous bosonic systems ϕ is just a constant for the liquid phase, while, for the solid phase it is a Nosanow product $\prod_i \varphi(r_i - R_i)$ where R_i are the lattice sites[3]. The factor F describes the correlations between the atoms and can be written in the so called *Feenberg form:*

$$F(\vec{r}_1 \cdots \vec{r}_N) = exp\{-\frac{1}{2}\sum_{i<j} u(r_{ij}) - \frac{1}{2}\sum_{i<j<l} u^{(3)}(\vec{r}_i, \vec{r}_j, \vec{r}_l) + \cdots\} \tag{1.6}$$

The two body term is the *Jastrow* term [4]while $u^{(3)}$ is referred to as the *triplet* term. The underlying hypothesis is that terms of order higher than the third are rapidly decreasing. In the variational approach one looks for the best pseudopotentials u, $u^{(3)}$. The simplest possible parametrization for the Jastrow term is the McMillan form[5]:

$$u(r) = \left(\frac{b}{r}\right)^m \tag{1.7}$$

This simple term allows already for a good description of short range correlations due to the repulsion between particles: the upper bound of the energy in ^{4}He is $E_{GS}^{var} = -5.72K$, within only a 10% of the potential and kinetic energy obtained with GFMC solutions. Inclusion of the triplet term considerably improves the energy, leading to a value $E_{GS}^{var} = -6.74K$, [6] and also th saturation density which is in very good agreement with the experimental data.

Recently Vitiello et al. [7], and Reatto et al. [8] ,[9] suggested a new variational

wave function that allows for a better description of ^{4}He than the pure Jastrow wave function. It consists on coupling particles via auxiliary degrees of freedom. This kind of trial wavefunction is referred to as *Shadow Wave Function (SWF)*. This wave function describes the system both in the liquid and in the solid phase and gives an upper bound for the variational energy that is lower than the value obtained with Jastrow or Jastrow +Nosanow wave functions, but higher than the value obtained adding the triplet terms in eq. 1.6 In section 2 we shortly review the

SWF formalism and the formulas to calculate observables. In section 3 we will sketch an outline of our project which consists in a different parametrization of the SWF by introducing a density dependence of the variational parameters in the SWF by with the goal of describing inhomogeneous systems. Section 4 and 5 will be devoted to the description of the preliminary results obtained with this new wave function.

2

Shadow Wave Functions

The Shadow trial wave function for a system of N particles is defined as:

$$\Psi_T = \int \Xi(R,S)dS = \tag{2.1}$$

$$= \exp\left(\sum_{i<j}\frac{1}{2}u_{pp}(r_{ij})\right)\int \exp\left(\sum_i u_{ps}(|\vec{r}_i - \vec{s}_i|)\right)\exp\left(\sum_{i<j}u_{ss}(s_{ij})\right)dS$$

where $i,j = 1\cdots N$. We use the original parametrization of the pseudopotential[10], namely:

$$\begin{aligned} u_{pp} &= \left(\frac{b_p}{r}\right)^{m_p} \\ u_{ps} &= -C\,|\vec{r}_i - \vec{s}_i|^2 \\ u_{ss} &= \left(\frac{b_{sh}}{r}\right)^{m_{sh}} \end{aligned} \tag{2.2}$$

Note that this parametrization of the shadow wave function contains five variational parameters that we will refer to as:

- b_p : particle-particle pseudopotential strength
- b_{sh} : shadow-shadow pseudopotential strength
- m_p : particle-particle pseudopotential exponent
- m_s : shadow-shadow pseudopotential exponent

- C : particle-shadow interaction strength

The energy expectation value is obtained introducing 2.2 in 1.1 to obtain the following expression:

$$E_{GS}^{var} = \int dRdS^l dS^r p(R, S^l, S^r) \frac{H\Xi}{\Xi} \tag{2.3}$$

where:

$$p(R, S^l, S^r) = \frac{\Xi(R, S^l)\Xi(R, S^r)}{\int dRdS^l dS^r \Xi(R, S^l)\Xi(R, S^r)} \tag{2.4}$$

and l , r stand for "*left*" and "*right*", the conventional names used to distinguish the two sets of shadow variables appearing in eq. 2.3. The attempted Metropolis move consits in a sequential random displacement of one particle in a cubic box of side Δ_p and of its own shadows in a box of side Δ_{sh}. Each move is accepted with probability:

$$P = \min\left(1, \frac{p_{new}(R, S, S')}{p(R, S, S')}\right) \tag{2.5}$$

The system practically consists of a "mixture" of three different kinds of species: real particles, 'left' shadows and 'right' shadows. This analogy has been recently developed in an appropriate way also in HNC formalism.

2.1 Calculation of observables

The observables monitored in our calculation are essentially three:

1. energy
2. order parameters to look for the actual phase of the system
3. two body distribution function $g(r) = \frac{1}{N\rho} \sum_{i \neq j} \langle \delta(|\vec{r}_i - \vec{r}_j - \vec{r}|) \rangle$

2.1.1 Energy

The main problem in the evaluation of the total energy of the system consits on the calculation of kinetic energy T (the potential energy is obtained simply averaging $\sum_{i<j} v_{ij}$ over all the configurations) In the case of a bosonic fluid described by a shadow wave function we have two different expressions for T. One of them is the

so called *Pandhariphande-Bethe* form, that comes out from the direct evaluation of $\sum_i \vec{\nabla}_i^2 \Psi/\Psi$:

$$\begin{aligned} T_{PB} &= \frac{\hbar^2}{4m}\langle \Xi(R,S^l)| \sum_i \sum_{j\neq i} \vec{\nabla}_i^2 u_{pp} \\ &+ \frac{1}{2}\left(\sum_{j\neq i} \vec{\nabla}_i u_{pp}\right)^2 + \left(\sum_{j\neq i} \vec{\nabla}_i u_{pp}\right)\cdot(\vec{\nabla}_i u_{pl}) \\ &+ \left(\sum_{j\neq i} \vec{\nabla}_i u_{pp}\right)\cdot(\vec{\nabla}_i u_{pr}) - \vec{\nabla}_i^2 u_{pl} - \vec{\nabla}_i^2 u_{pr} \\ &+ \left(\vec{\nabla}_i u_{pl}\right)^2 + \left(\vec{\nabla}_i u_{pr}\right)^2 |\Xi(R,S^r)\rangle \end{aligned} \tag{2.6}$$

Another widely used estimator for T is the so called *Jackson-Feenberg* kinetic energy, based upon the Jackson-Feenberg identity. The outcome is an identity that allows us to replace some terms involving particle shadow interaction. The final expression is:

$$\begin{aligned} T_{JF} &= \frac{\hbar^2}{4m}\langle \Xi(R,S^l)| \sum_i -\frac{1}{2}\sum_{j\neq i} \vec{\nabla}_i^2 u_{pp} \\ &- \frac{1}{2}\vec{\nabla}_i^2 u_{pl} - \frac{1}{2}\vec{\nabla}_i^2 u_{pr} + \frac{1}{2}\left(\vec{\nabla}_i u_{pl}\right)^2 + \frac{1}{2}\left(\vec{\nabla}_i u_{pr}\right)^2 \\ &- \left(\vec{\nabla}_i u_{pl}\right)\cdot\left(\vec{\nabla}_i u_{pr}\right) |\Xi(R,S^r)\rangle \end{aligned} \tag{2.7}$$

Comparison between PB and JF kinetic energies gives informations about the equilibration of the system. In fact this two estimators must lead at the same mean value. Usually T_{JF} has a smaller variance than T_{PB}, but if we consider the *total energy* $< E >=< T > + < V >$ it comes out that the use of PB expression gives a smaller variance. The computation of both the estimators is very useful.

2.1.2 Order parameters

For every possible application of the formalism it is essential to calculate proper order parameters telling us if we are in a crystalline or in a liquid -like phase. The

order parameter we have chosen is the first term of the Fourier transform of the one-body density[11]. Its value on a single configuration is given by:

$$\rho^{INST}_{\{\vec{G}\}} = \frac{1}{N m_{\{\vec{G}\}}} \sum_{\substack{i=1 \\ G\in\{\vec{G}\}}}^{N} e^{i\vec{G}\cdot\vec{r}_i} \tag{2.8}$$

where $\left\{\vec{G}\right\}$ denotes a 'star' of vectors in the reciprocal lattice and m is the multiplicity of the star. This order parameter checks if the positions of the atoms tend to stay around the crystalline sites (in our case we are monitoring the fcc crystal) or if they are in a more disordered phase. In the first case the value of q is little less than one, in the second it fluctuates approximately around zero It is customary to average over all the configurations taking the modulus of $\rho^{INST}_{\{\vec{G}\}}$

$$\rho^{ACC}_{\{\vec{G}\}} = \langle|\rho^{INST}_{\{\vec{G}\}}|\rangle \tag{2.9}$$

This order parameter takes again a value a little lower than 1 in the solid, while in the liquid it fluctuates around $1/\sqrt{N}$. The order parameter defined in 2.9 is the quantity effectively accumulated in our numerical code.

2.1.3 Two body correlation function

In a particle-shadow mixture one can look for several two body correlation functions. In particular one has:

- $g_{pp}(r)$: particle-particle correlation function
- $g_{ss}(r)$: shadow-shadow correlation function
  (only between shadows of the *same* kind)
- $g_{ps}(r)$: particle-shadow correlation function
- $g_{s^l s^r}$: shadow-shadow correlation function
  (between shadows of *different* kind)

3

Outline of the project

3.1 Results in ^{4}He

Much work have been done to compute variational with SWF energies both in solid and liquid ^{4}He. Earlier calculation used quite exclusively a McMillan form for the shadow-shadow pseudopotential. In table 3.1 we report a summary of the energies obtained and the relative values for the variational parameters The results in the liquid seem to be not as good as those obtained using a Jastrow + Triplet (J+T) trial wave function, but improve significantly the pure Jastrow (J) case (see table 3.2) .

We want to stress the fact that the solid and the liquid are described with the *same* wave function. This is an interesting feature in particular for the solid phase, for which no Nosanow factor has been used. The correlation hole described by

$\rho\sigma^3$	Energy	b_p	b_{sh}	m_{sh}	C
0.365	-6.061±0.025	1.13	1.40	5	4.0
0.365	-6.241±0.035	1.13	1.20	9	4.0
0.365	-6.133±0.048	1.13	1.16	12	4.0
0.438	-5.360±0.035	1.12	1.55	5	4.0
0.491	-5.004±0.055	1.10	1.70	5	4.8
0.550	-3.521±0.032	1.10	1.67	5	5.7
0.550	-3.529±0.027	1.10	1.35	9	5.7
0.550	-3.563±0.031	1.09	1.28	12	5.7

Table 3.1: Variational energies obtained with shadow wave function and relative parameters from ref. [10]

Trial w.f.	$\rho\sigma^3$	Energy
J	0.365	-5.717±0.021
J+T	0.365	-6.674±0.007
JN	0.550	-3.322±0.019
JN+T	0.550	-3.786±0.014

Table 3.2: Variational energies obtained with several trial wave functions. J: pure Jastrow; J+T : Jastrow+Triplet. N: Nosanow (for solid) from ref. [10]

shadows seems to provide by itself a mechanism of confinement of the system on a crystalline structure when periodic boundary conditions are used. To achieve a good description of the system one just needs to change the parameters according to the given density. Several results have been obtained also at the freezing and the melting density evaluated with GFMC ($\rho = 0.438$ and $\rho = 0.491$ respectively) As one can immediately note there are some parameters that seem not to depend so strongly by the density. In particular the variation of b_p is small. On the contrary the variation of b_{sh} and C with the density is wider. Results obtained at freezing and melting density (see table 3.1) confirms this trend.
More recent results obtained with a better parametrization of u_{ss} leads to a better value for the energy upper bound($E = -6.69K$)[14].

3.2 Unique wave function for solid and liquid phase

Previous analysis suggests the possibility to find some useful parametrization of the SWF to describe at the same time the system at different densities. One need to introduce a density dependence on the variational parameters, making the wave function depending from the density itself. One of the first question to ask is which are the parameters to fix and which to vary. The results discussed in following sections address this question.
Let us assume that the only density dependent parameter is b_{sh}. The dependence from the density is taken to be of the form:

$$b_{sh} = b_0 + \frac{1}{2} b_1 (c_i + c_j) \tag{3.1}$$

where:

$$c_i = \frac{1}{A}\sum_l \nu(|\vec{s}_i - \vec{s}_l|) \tag{3.2}$$

and $\nu(r)$ is taken to be a Fermi distribution:

$$\nu(r) = \frac{1}{e^{\mu(r^2-R^2)}+1} \tag{3.3}$$

Here A is a normalization factor:

$$A = 4\pi \int_0^\infty dr r^2 \nu(r) \tag{3.4}$$

and R and μ are the *cutoff* and *slope* parameter. The local density is given by the operator c_i, counting the number of shadows lying in a spherical region centered on the i-th shadow . In an elementary Metropolis move of a particle we choose the value of b_{sh} according to eq. 3.1 measuring the density around the i-th and j-th particle and then averaging. The wave function becomes sensible to the local situation of the system, making in principle possible the description of both homogeneous and inhomogeneous systems. Alternative choices to eq. 3.1 can also be made. For instance $b_{sh} - b_0$ can be taken of the form $b_1\sqrt{c_i c_j}$. The aim of this parametrization is the study of systems with coexistent phases such as solid-liquid interfaces in ^{4}He. The realization of an interface is possible for values of density between the between the freezing and the melting densities. The simulation should start filling half a box with a solid configuration and half with a liquid configuration. Then the system will be allowed to evolve. The dependence of the wave function from the local density would permit the creation of a stable smooth density profile, provided that the system is within an appropriate range of densities. Many points, such as the choice of periodic boundary conditions, the detailed setup of the initial conditions, the choice of the density itself, belong to a next step of the project. The first thing to do is to verify how well this wave function can work in homogeneous systems, and what kind of refinements are required to get good results.

4

Optimization of b_{sh}

Determination of the explicit form for the dependence of b_{sh} on the density is the first step to be done . There are several techniques to optimize parameters in a variational wave function[12]. A preliminary study of the problem suggested us to proceed simply with a scan of the parameters over an appropriate range of values using the original SWF. The results are then fitted to get the value of the parameter minimizing the energy.

4.1 Preliminary results

Calculations were done at three different values of density:

- 0.365 equilibrium density for liquid
- 0.438 freezing density
- 0.550 solid density

Fixed parameters are $b_p = 1.12$, $m_p = 5$ and $m_{sh} = 9$. For each value of density we tried also three values of C: 4.0, that is a good value for liquid density,5.7 that is a good value for solid and the intermediate value of 4.8. All the runs were performed starting from a fcc lattice both for particles and shadows. Equilibration consisted of 2500 Monte Carlo steps, while averaging was made over 10000 Monte Carlo steps. Statistical errors were computed from the variance and from an estimate of the autocorrelation time estimated by the block variance method of Jacucci and Rahman [13]. Autocorrelation time does never exceed 10 MC steps.

C	$b_{sh.opt}$	$\Delta b_{sh.opt}$	E_{var}	ΔE_{var}	tolerance	
4.0	1.21	0.11	-6.17	0.04	1.09	1.31
4.8	1.13	0.09	-6.13	0.05	1.04	1.21
5.7	1.05	0.06	-6.19	0.05	0.99	1.10

Table 4.1: Best values of b_{sh} , tolerances and correspondent energies in K obtained by the fits in fig. 4.1, 4.2 and 4.3 with relative error, at liquid density

C	$b_{sh.opt}$	$\Delta b_{sh.opt}$	E_{var}	ΔE_{var}	tolerance	
4.0	1.35	0.08	-5.46	0.05	1.27	1.43
4.8	1.28	0.06	-5.51	0.04	1.21	1.34
5.7	1.18	0.07	-5.33	0.03	1.11	1.25

Table 4.2: Best values of b_{sh} , tolerances and correspondent energies in K obtained by the fits in fig. 4.4, 4.5 and 4.6 with relative error at freezing density

4.1.1 Liquid Density

The results for liquid are shown in fig. 3.1, 3.2 and 3.3. The energy as a function of b_{sh} shows a minimum for all the values of C considered. We note that as expected the minimum lies in the region where the system is in a liquid phase. The energy shows a jump in correspondence of a critical value of $b_{sh} = 1.5$ where the system is in a solid phase (see *e.g.* ref. [15]. The fit was performed using a cubic polynomial:

$$a_0 + a_1 x + a_2 x^2 + a_3 x^3 \tag{4.1}$$

The fit was performed in the region where the system is in the same phase. In table 4.1 we report for each value of C considered the optimal value of b_{sh}, the minimum of the energy, the corresponding error and the extremes of tolerance for $b_{sh.opt.}$ intended as the range of values in which the energy varies less than 2σ where σ is the statistical error on the energy obtained by the simulation.

4.1.2 Freezing Density

Results are shown in fig. 4.4, 4.5, 4.6. Similarly to the liquid case, at the freezing density we have always a minimum of the variational energy moving b_{sh} In this case we notice that the case with $C = 4$ presents different behaviour from the other two cases. The minimum of the energy is between the solid and the liquid phase, while for greater values of C the minimum is found in the liquid phase. Also the jump in

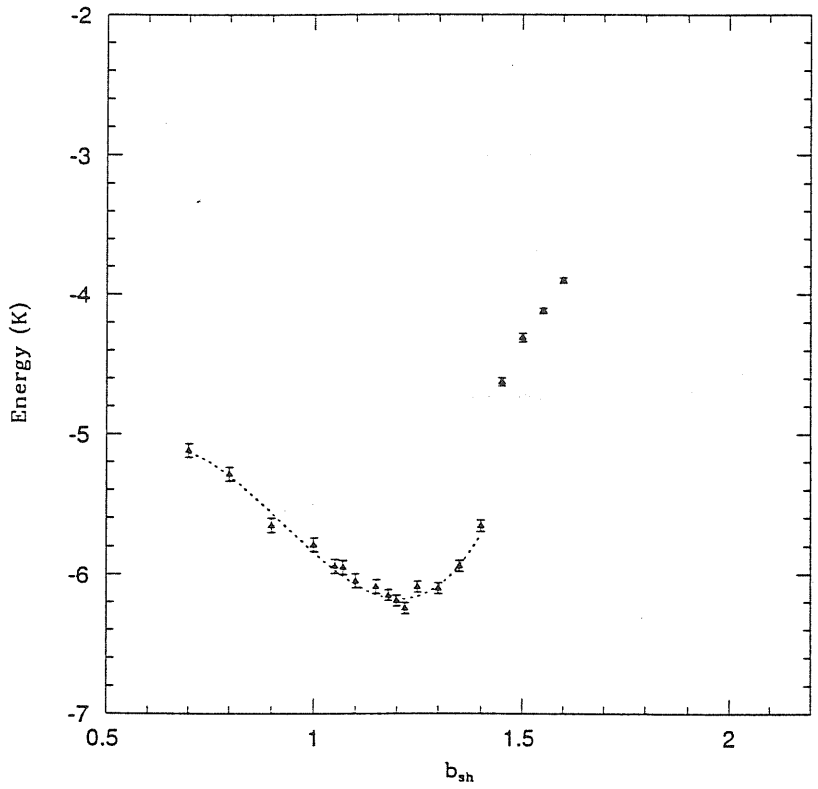

• **Fig. 4.1** Variational Energy as a function of the variational parameter b_{sh} for $C = 4.0$ at density $\rho = 0.365$. Filled triangles: liquid; Empty triangles: solid. Dashed line: cubic polinomyal fit (see text).

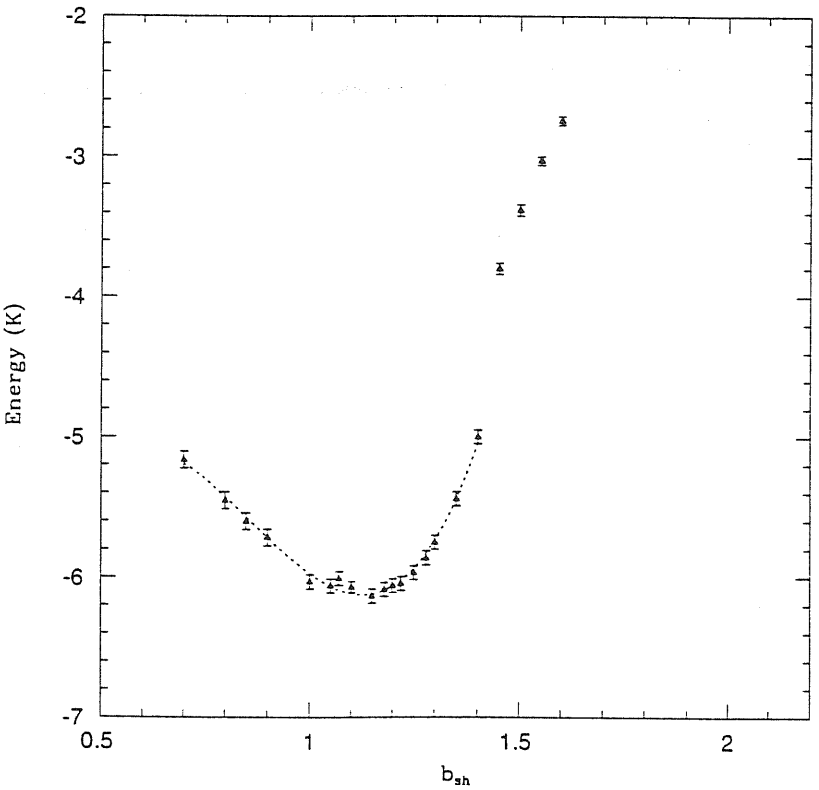

• **Fig. 4.2** Variational Energy as a function of the variational parameter b_{sh} for $C = 4.8$ at density $\rho = 0.365$. Filled triangles: liquid; Empty triangles: solid. Dashed line: cubic polinomyal fit (see text).

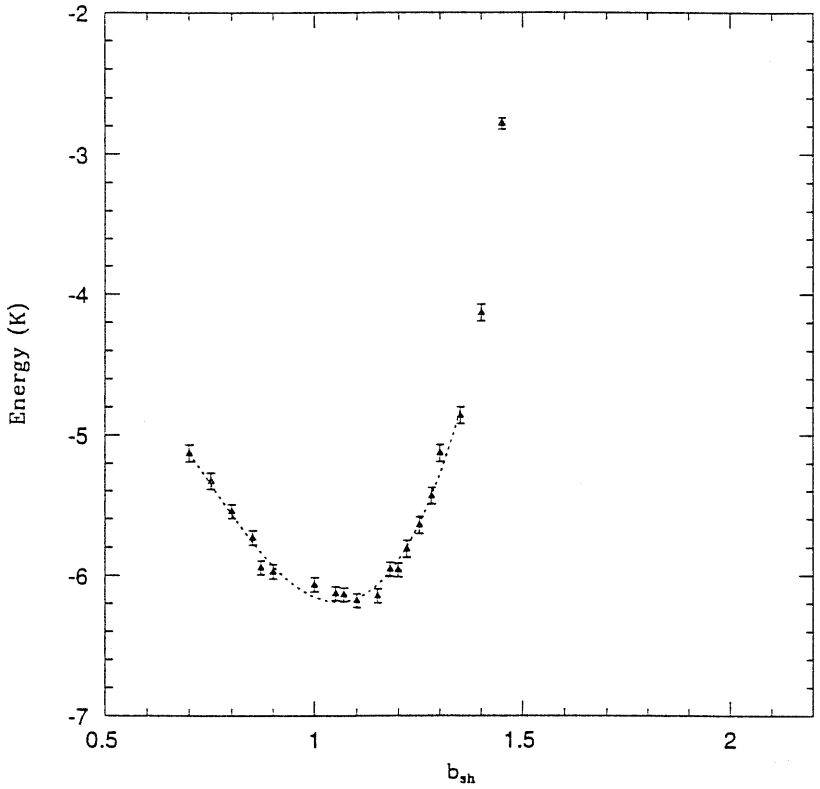

- **Fig. 4.3** Variational Energy as a function of the variational parameter b_{sh} for $C = 5.7$ at density $\rho = 0.365$. Filled triangles: liquid: Empty triangles: solid. Dashed line: cubic polinomyal fit (see text).

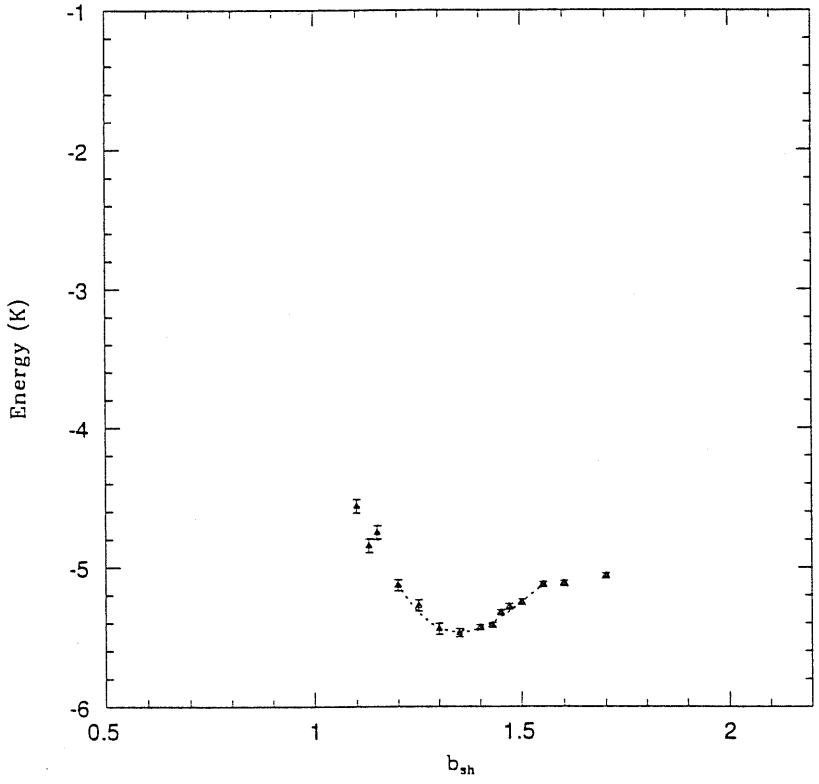

- **Fig. 4.4** Variational Energy as a function of the variational parameter b_{sh} for $C = 4.0$ at density $\rho = 0.438$. Filled triangles: liquid: Empty triangles: solid. Dashed line: cubic polinomyal fit (see text).

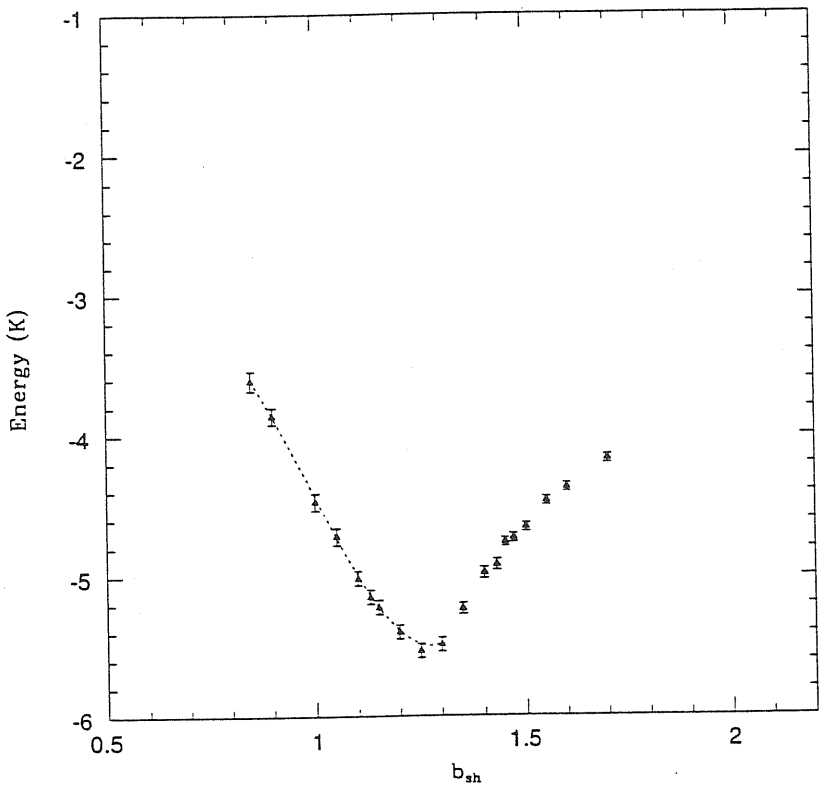

- **Fig. 4.5** Variational Energy as a function of the variational parameter b_{sh} for $C = 4.8$ at density $\rho = 0.438$. Filled triangles: liquid; Empty triangles: solid. Dashed line: cubic polinomyal fit (see text).

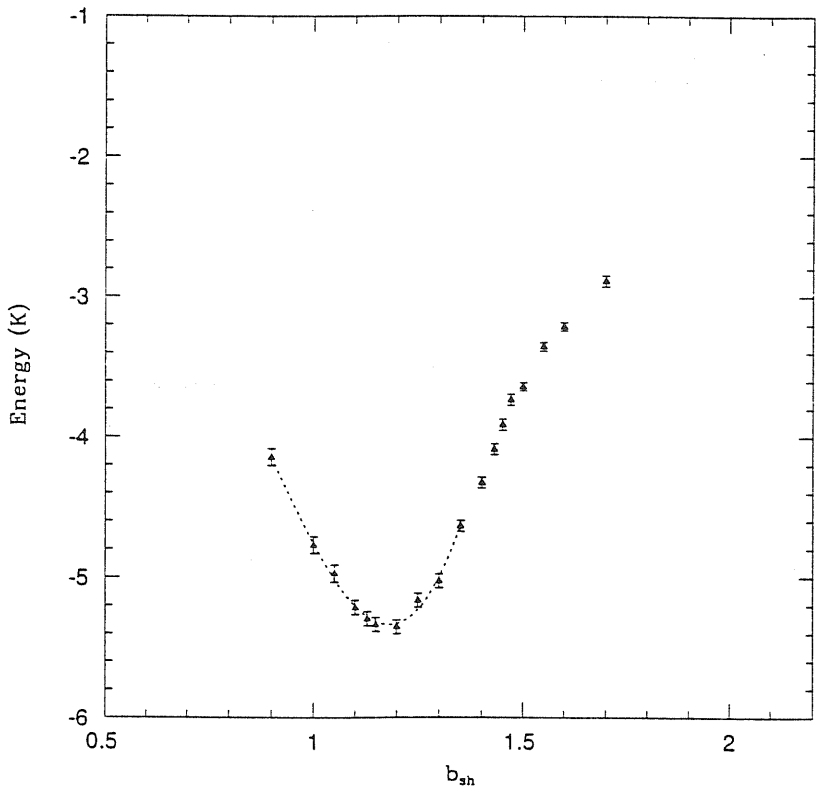

- **Fig. 4.6** Variational Energy as a function of the variational parameter b_{sh} for $C = 5.7$ at density $\rho = 0.438$. Filled triangles: liquid; Empty triangles: solid.

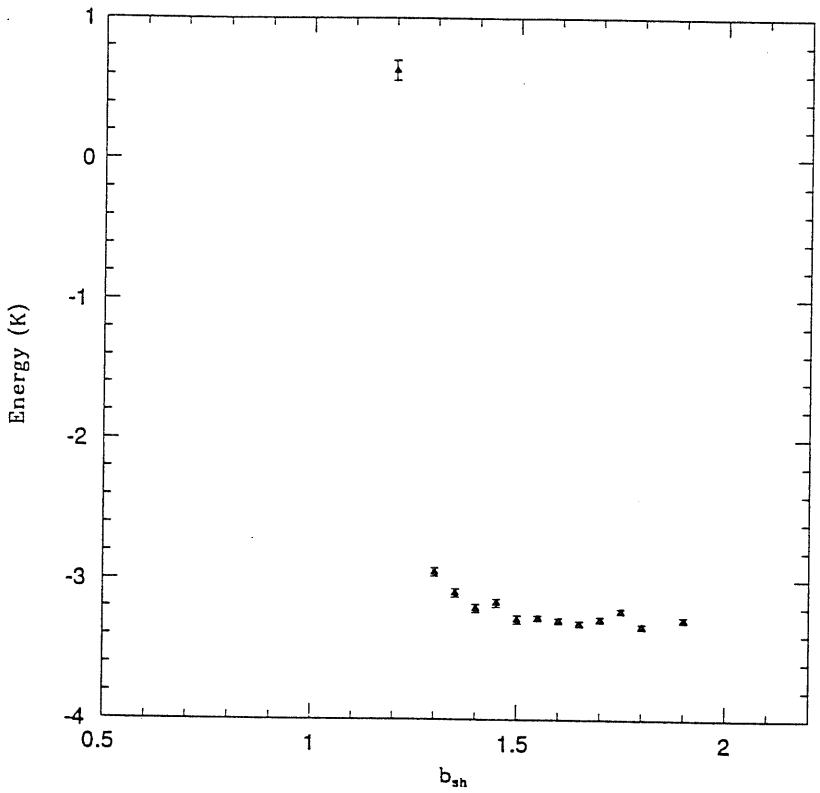

• **Fig. 4.7** Variational Energy as a function of the variational parameter b_{sh} for $C = 4.0$ at density $\rho = 0.550$. Filled triangles: liquid; Empty triangles: solid.

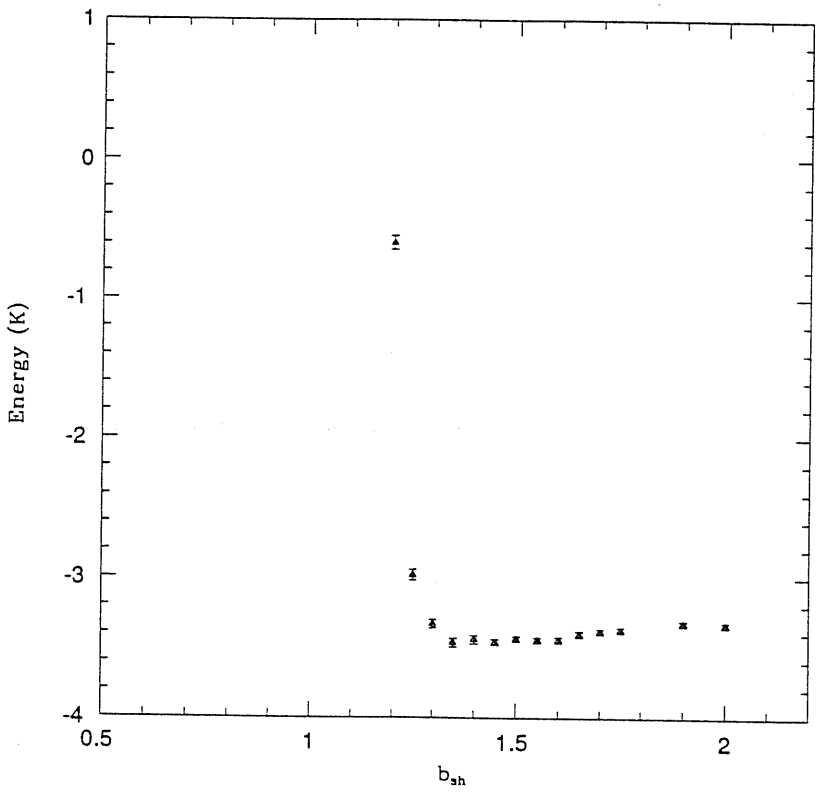

• **Fig. 4.8** Variational Energy as a function of the variational parameter b_{sh} for $C = 4.8$ at density $\rho = 0.550$. Filled triangles: liquid; Empty triangles: solid.

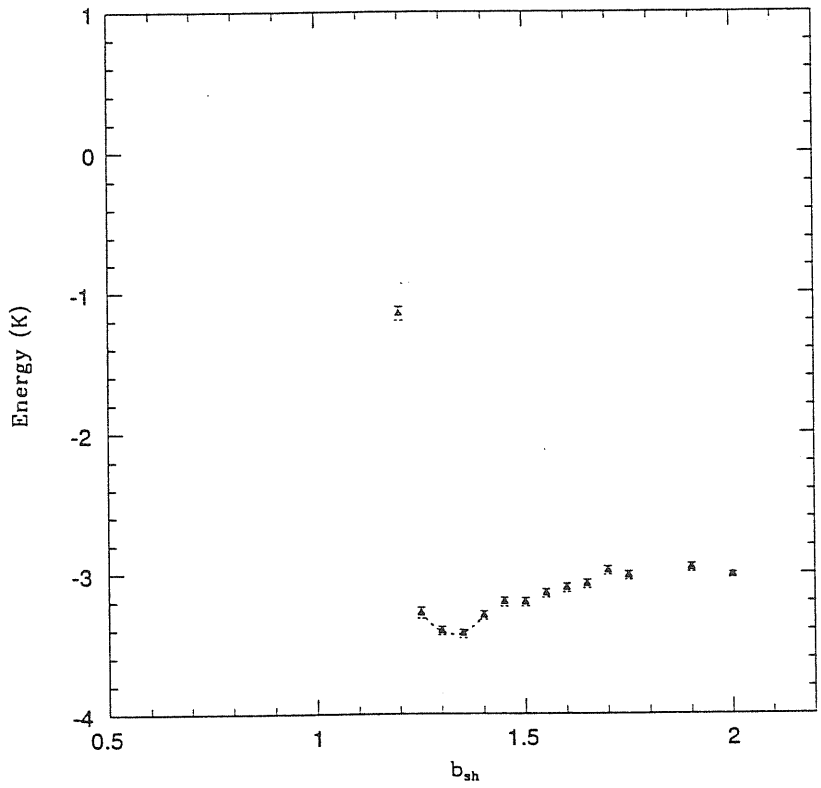

- **Fig. 4.9** Variational Energy as a function of the variational parameter b_{sh} for $C = 5.7$ at density $\rho = 0.550$. Filled triangles: liquid: Empty triangles: solid. Dashed line: quadratic polinomyal fit (see text).

C	$b_{sh.opt}$	$\Delta b_{sh.opt}$	E_{var}	ΔE_{var}	tolerance	
4.0	*1.70	0.30	-3.30	0.03	1.50	$\geq$2.00
4.8	*1.45	0.10	-3.40	0.03	1.35	1.65
5.7	1.33	0.05	-3.44	0.03	1.28	1.38

Table 4.3: Best values of b_{sh} , tolerances and correspondent energies in K (see fig 4.7, 4.8 and 4.9) with relative error at solid density. Points indicated with * do not correspond to real minima and tolerances corresponds to the half width of the region of minimum of energy

energy between liquid and solid phase is wider for higher values of C. This shows how the dependence by this parameter is determinant in driving the behaviour of the system. Also in this case the fits were performed with a cubic polinomyal in all cases. Energies and coefficients are reported in table 4.2. Note that freezing density does not coincide with the melting one (for ^{4}He $\rho_{melting} = 0.491$). At this density the system is in a liquid phase, and this explains why the minimum lies always under the critical value of b_{sh}

4.1.3 Solid Density

Results are shown in fig. 4.7, 4.8, 4.9. The behaviour at solid density is completely different from the previous cases. The variational energy does not show any minimum for the lowest values of C. For $C = 4$ the system seems to approach from above some constant value. This makes the tolerance on the 'best' value of b_{sh} very high. Nevertheless the variational energy is quite high with respect to the best values obtained with $C = 5.7$, where the curve develops a clear minimum. Results are reported in table 4.3. The fit in this case was made with a parabola. The value of Δ_{sh} necessary to get a given acceptance ratio provides a qualitative measure of the diffusion of the shadows. As b_{sh} increases we find lower and lower values for Δ_{sh}, meaning that we are approaching the Nosanow limit.

4.2 b_{sh} as a function of density

The results of the previous section make it possible to determine the form of the dependence of the variational parameter b_{sh} on the density. First of all we have to check if the linear dependence assumed in 3.1 is compatible with the results. In fig.

C	b_0	b_1
4.0	0.51	1.91
4.8	0.39	2.02
5.7	0.53	1.46

Table 4.4: Parameters b_0 and b_1 fitted by data of preceeding section

4.10, 4.11 and 4.12 we report the optimal value of b_{sh} as a function of the density for the three values of C considered with the respective tolerances. In the cases where there is no minimum of the energy at solid density we report only the tolerance, intended as the width of the region where energy assumes a quite constant value. As one can easily see, the points are compatible with a linear dependence, making possible a first check of the method with the use of the formulas of the previous chapter. The coefficients b_0 and b_1 defined in 3.1 obtained in this way are written in table 4.4.

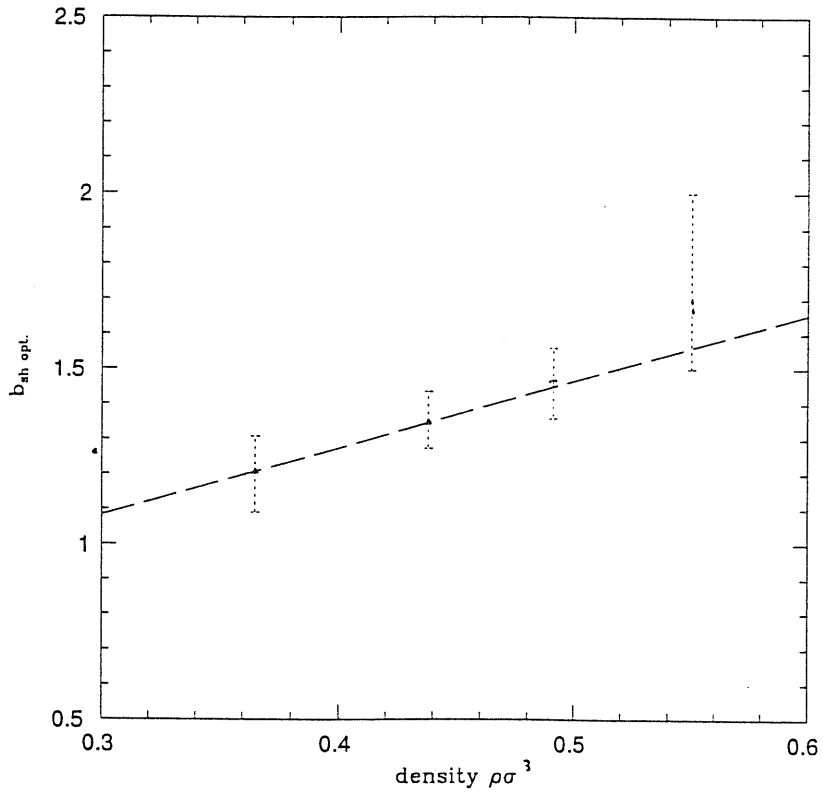

• **Fig. 4.10** Optimized value of b_{sh} vs. density for $C' = 4.0$ and relative tolerances. Dashed line: linear fit. Empty circle: value of $b_{sh.opt}$ obtained by SWF+LDO at $\rho = 0.491$ (see text).

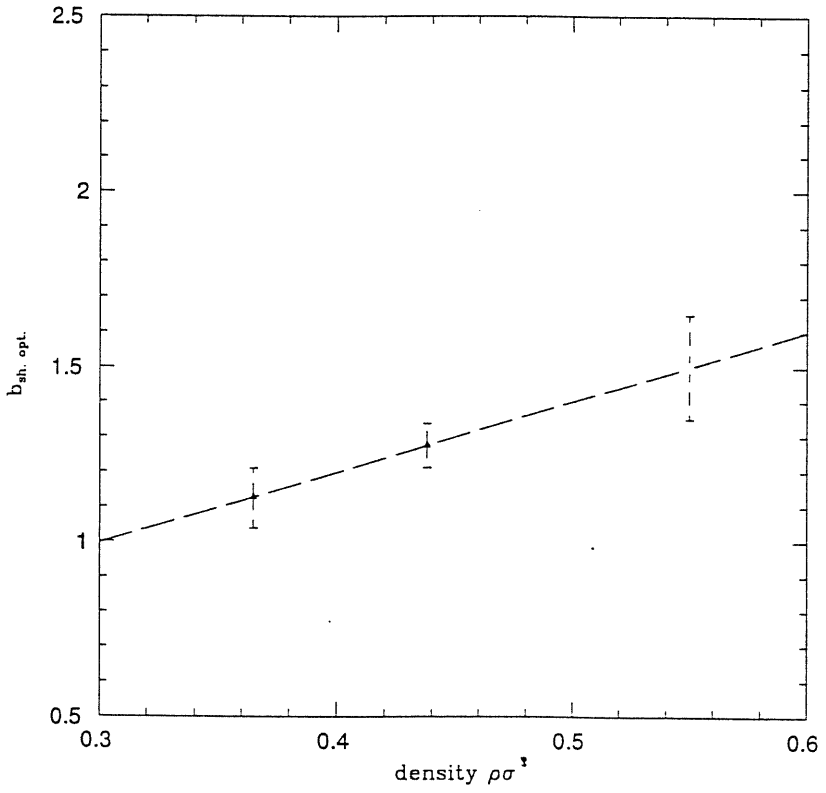

• **Fig. 4.11** Optimized value of b_{sh} vs. density for $C' = 4.8$ and relative tolerances. Dashed line: linear fit

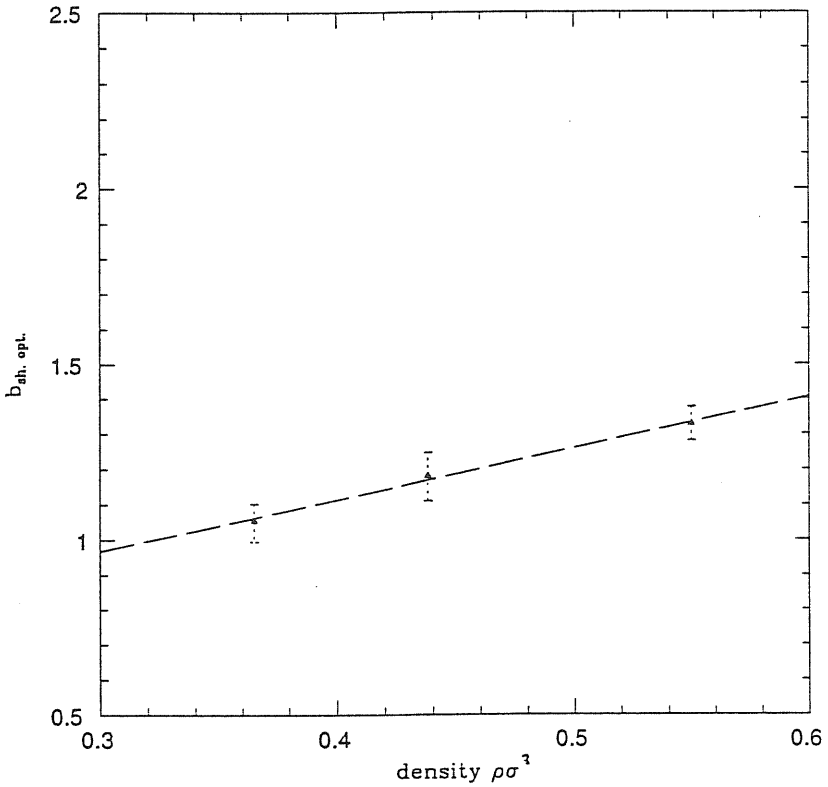

• Fig. 4.12 Optimized value of b_{sh} vs. density for $C = 4.8$ and relative tolerances. Dashed line: linear fit

5

Estimating the Density Operator

In this section we report about the first tests performed using the method presented in section three. We have checked is the efficiency of the algorithm in an *homogeneous* system. An analysis was performed at four different values of density: the three values checked before and the melting density ($\rho = 0.491$). Keeping C fixed we have only to change the part relative to the acceptance of the move because the calculation of the estimators does not involve the pseudopotential u_{ss}. The introduction of other parameters dependent by the density would also affect the computation of estimators. A last remark must be done about the parameter μ . Its value was taken equal to 3, and kept fix during all the simulations. This value provides a sufficiently steep function in the region of the cutoff. Some change should happen with low values of μ that can make smoother the function. This point has not yet been explored.

5.1 Efficiency of the Density Operator

One of the first requirements on this density operator is to reproduce the homogeneous case. At the beginning we must choose some reasonable values for the cutoff R of the function $\nu(r)$ defined in the previous chapter. In order to reproduce the correct density of the system a possible choice is to put the cutoff at the first minimum of the $g(r)$ correspondent to the density explored. This should ensure that we are counting all the shadows contained into the first shell of neighbours. It is customary to introduce the *mean parameter of the configuration* defined as:

$$\overline{b}_{sh} = b_0 + b_1\overline{c} \tag{5.1}$$

where

$$\overline{c} = \frac{1}{2N} \sum_{a} \sum_{i=1}^{N} c_i^a \tag{5.2}$$

where N is the number of shadows of each kind in the simulation, a is *left* or *right* and the c_i are defined in the previous chapter. This quantity is to be averaged over all the configurations. This estimator allows us to control the average of the local density corresponds to the macroscopical average density. A proper choice of the cutoff makes the two value really close each other, ensuring that the value of $\overline{b}$ is near the optimal one.

5.1.1 mean values and variances

In fig 5.1 and 5.2 we report the running average value of $\overline{c}$ together with the instantaneous values for two different densities $\rho = 0.365$ and $\rho = 0.438$. As one can see the equilibrium value is quickly reached. Autocorrelation time for this quantity is of about 200 MC steps (we must notice that c is a *classical* quantity). We want to stress the fact that fluctuations of $\overline{c}$ which is a *averaged value over the configuration* are different from the fluctuations of c_i, which are really important in determining the energy.

5.1.2 comparison with standard SWF

In table 5.1 we report the results obtained with standard SWF. The main outcomes are two. First we notice that results at liquid,solid and melting densities are quite in agreement with the old ones. We must also notice that at the freezing density we find that the energy is higher than in standard SWF. If we look at the variance of the local density *of the particle* $\sigma^2(c_i)$, that is $N^2\sigma^2(\overline{c})$, we notice that it is larger here than at liquid or melting density (see table 5.1). This implies that during the simulation we sample configurations with higher energy (corresponding to values of b_{sh} far from the running mean value). The outcome is a bad worsening of the total energy. The reason for which the variance is higher is probably that in the system at that density there are still present solid seeds growing and melting continuously and creating regions where the local density assumes values far from the mean. This hypothesis would explain also the behaviour of the order parameter whose mean value does never reach the typical value of the molten system, but looks to assume

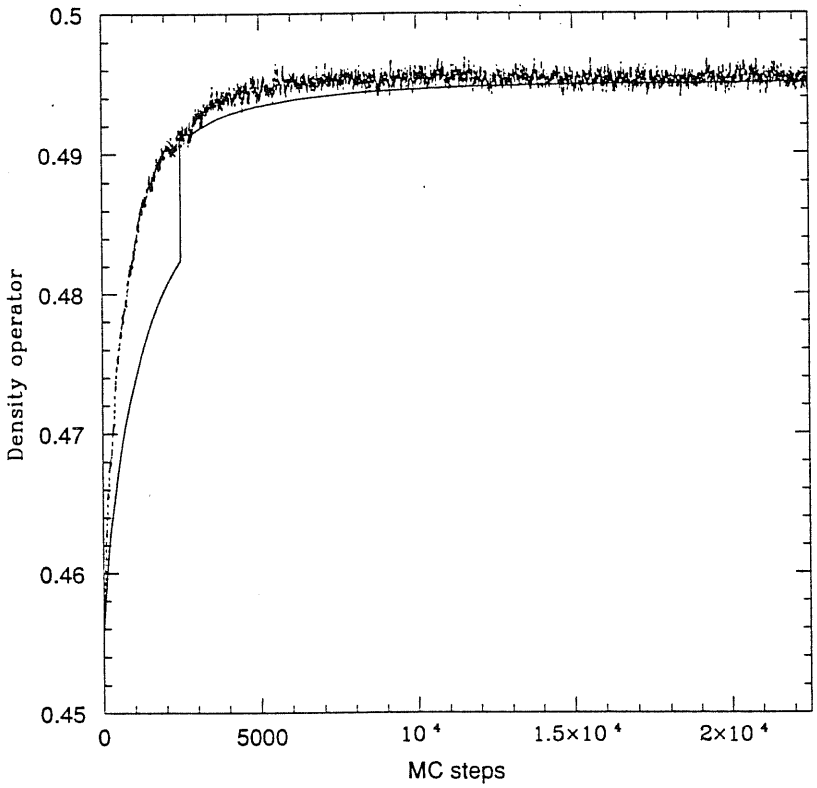

• **Fig. 5.1** Run time average and instantaneous values of $\bar{c}$ at liquid density.

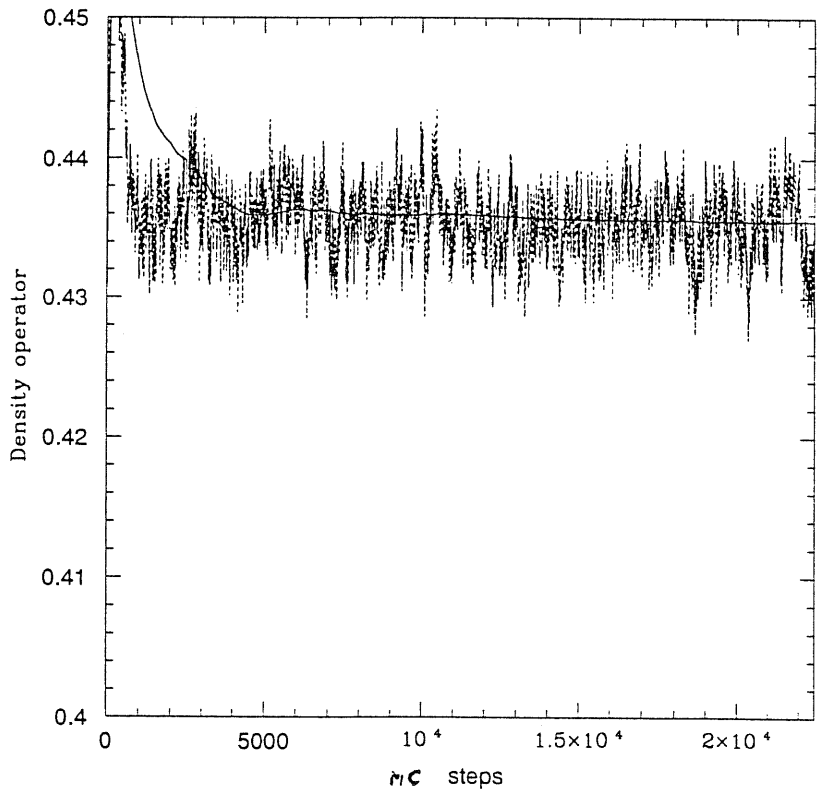

• **Fig. 5.2** Run time average and instantaneous values of $\bar{c}$ at freezing density.

$\rho\sigma^3$	R	E_{var}^{SWF}	$E_{var}^{SWF+LDO}$	$\langle\overline{c}\rangle$	$\sigma^2(c_i)$
0.365	2.1	-6.17±0.05	-6.23±0.05	0.3671±0.0006	0.0379
*0.438	1.9	-5.39±0.04	-5.01±0.05	0.4364 ±0.0005	0.0807
0.491	1.9	**-4.96±0.03	-4.93±0.04	0.4964 ±0.0002	0.0155
0.550	1.8	-3.28±0.03	-3.20 ±0.04	0.5313 ±0.0006	0.1121

Table 5.1: Variational energies obtained with SWF+Local Density Operator (LDO) compared with the fit of standard SWF results with the same value of $\overline{b}$. The values of parameters are $b_0 = 0.51$, $b_1 = 1.91$. R is the cutoff in the function $\nu(r)$.
* computed with $b_0 = 0.46$
** result of direct simulation

R	E_{var}	$\langle\overline{c}\rangle$	$\sigma^2(c_i)$
1.80	-5.87±0.05	0.3738 ±0.0006	0.0787
2.10	-6.23±0.05	0.3671 ±0.0003	0.0379
2.60	-6.17±0.05	0.3566 ±0.0003	0.0208
3.40	-6.22±0.05	0.3637 ±0.0003	0.0172

Table 5.2: Variational energies obtained with different values of cutoff R at liquid density $\rho\sigma^3 = 0.365$, and values of $\overline{c}$ and variances relative to c_i

higher values. One way to reduce the variance on the local density is to increase the value of the cutoff, because in such a way the fluctuations of the number of particles included in the region considered normalized to the volume becomes smaller. This is exploited in table 5.2 where some results obtained at liquid density with four different values of the cutoff are reported. The values of R for which $\overline{c}$ is closer to the density ρ are those corresponding to the minima of th $g(r)$. For instance that the choice of the cutoff at $R = 2.6\sigma$ gives a smaller variance than for $R = 2.1\sigma$, but $\overline{c}$ is worse, giving a little higher energy. A simulation performed at freezing density with the same parameters reported in table 4.4 but with a value of $R = 3.4$ (close to the second minimum of the $g(r)$) gives the correct variational energy $E_{var} = -5.36\pm0.05$

R	E_{var}	$\langle\overline{c}\rangle$	$\sigma^2(c_i)$
1.80	-3.20±0.04	0.5313 ±0.0006	0.1121
2.20	-3.25±0.03	0.4789 ±0.0001	0.0042
2.80	-3.20±0.03	0.5578±0.0001	0.0038

Table 5.3: Variational energies obtained with different values of cutoff R at solid density $\rho\sigma^3 = 0.550$, and values of $\overline{c}$ and variances relative to c_i

b_0	E_{var}	$\langle\overline{c}\rangle$	$\langle\overline{b}_{sh}\rangle$	phase
0.41	-4.79 ±0.07	0.436	1.24	liquid
0.46	-5.01 ±0.06	0.436	1.29	liquid
0.51	-5.27 ±0.05	0.436	1.34	liquid
0.56	-5.28 ±0.05	0.435	1.39	liquid
0.61	-5.29 ±0.05	0.434	1.43	liquid
0.66	-4.14 ±0.04	0.467	1.55	solid
0.71	-4.05 ±0.04	0.465	1.60	solid

Table 5.4: Energy, $\langle\overline{c}\rangle$ and $\langle\overline{b}_{sh}\rangle$ at freezing density. Phases are obtained by order parameters described in section 2.

b_0	E_{var}	$\langle\overline{c}\rangle$	$\langle\overline{b}_{sh}\rangle$	phase
0.41	-3.52 ±0.06	0.477	1.32	liquid
0.46	-4.95 ±0.05	0.496	1.41	solid
0.51	-4.92 ±0.05	0.496	1.46	solid
0.56	-4.94 ±0.05	0.495	1.50	solid
0.61	-4.86 ±0.05	0.491	1.55	solid

Table 5.5: Energy, $\langle\overline{c}\rangle$ and $\langle\overline{b}_{sh}\rangle$ at melting density. Phases are obtained by order parameters described in section 2.

with a variance on $\overline{c}$ of 2.2×10^{-6}, less than one half of the previous value. Another argument confirming this strong dependence of the results from the variance of c_i is the results obtained at solid density, where the variance is higher. The tolerance in this case is wide, and the energy does not result to be affected by fluctuations in a dramatic way, even it is still worse than standard SWF calculation. In solid wide variances in c_i disturb the dynamic of shadows making them more rigid. Also in this case higher values of the cutoff give very good variances (see table 5.3).
Another important point is the comparison of the autocorrelation times, here calculated with the block variance method referred to in the previous section. Standard SWF calculations have values of the autocorrelation time is of the order of 5-6 MC steps while with the introduction of the local density this value goes to 10 - 20 MC steps.

5.2 Dependence from b_0

In table 5.4 and 5.6 we report some values obtained varying the coefficient b_0 around the value obtained fitting the minima of the energy as a function of b_{sh}. Calculations were made at the freezing and at the melting density. There is a flat region in both cases. At freezing density the system shows a minimum in the region of the liquid, with the , while at the melting density the system is in the solid state. As done before we can obtain from this data an "optimal" value of b_0 with a tolerance defined in this case as the width of the plateau. We can compare this value with the value predicted by the linear dependence obtained before. The result is in agreement with the value predicted by the linear law for b_{sh}.

6

Conclusions

The results obtained up to now clearly indicate that the parameter b_{sh} in eq. 3.1 has a linear dependence on the density for all the phases. Moreover the use of the density ρ as an "operator" in $b_{sh} = b_0 + b_1\hat{\rho}$ leads to results very similar to those obtained with the standard parametrization. There are however some points that have to be considered.

First of all the use of the local density operator increases the autocorrelation time for the energy. This implies that the computational effort required to achieve significative results is almost twice heavier than in the case in which the density is a constant parameter. Secondly, the strong dependence of the results on the cutoff parameter R appears to be a difficulty. For intermediate values of R ($R \leq \frac{1}{2}L$ where L is the length of the simulation box) one obtains quite different results whether R corresponds to a maximum or to a minimum of the pair correlation function $g(r)$. The best value of R corresponds to the minimum of the $g(r)$, which however depends upon the density of the system. Obviously the dependence upon R becomes weaker and weaker as R increases, but too large values of R may be not practical to study inhomogeneities of the system, and in any case they would require very large boxes.

It seems to be extremely important to keep under control the variance of the local density over all the range covered by the system at the coexistence density so that further optimization of the wave function seems to be necessary.. One possible improvement could be the introduction of a mechanism of adjustment of the cutoff based on the mean value of the local density estimated every some number of steps, according to a proper density dependence law. The method, if working,

can be extended to self-bounded system, such as clusters or free surfaces, by the introduction of a different form the shadow-shadow pseudopotential containing an attractive part[9].

Acknowledgments

Inspiration and fundamental indications for the development of this work are due to L.Reatto. I want to acknowledge together with the supervisor A.Ferrante and A.Belic for continuous collaboration and material help in the realization of this first part of the project.

References

[1] R.A.Aziz, V.P.S.Nain, J.S. Carley, W.L. Taylor, G.T. McConville : *J. Chem. Phys.* **70**, 4330 (1979).

[2] K.E. Schmidt, D.M. Ceperley: *Monte Carlo Techniques for Quantum Fluids, Solids and Droplets*, in *The Monte Carlo Method in Condensed Matter Physics*, Vol. 71 of *Topics in Applied Physics*, edited by K. Binder (Springer, Berlin,NY 1992), chap. 7.

[3] L.H. Nosanow: *Phys. Rev. Lett.* **13**, 270 (1964).

[4] R. Jastrow: *Phys. Rev.* **98**, 1479 (1955).

[5] W.L. McMillan: *Phys. Rev.* **138A**, 442 (1965).

[6] K. Schmidt, M.H.Kalos, M.A.Lee, G.V.Chester *Phis. Rev. Lett.* **45**, 573 (1980); **47**, 807 (1981).

[7] S. Vitiello, K. Runge, M.H. Kalos *Phys. Rev. Lett* **60** 1970 (1988).

[8] L. Reatto, G. L. Masserini: *Phys. Rev. B* **38**, 4516 (1988).

[9] L. Reatto: *On Shadow Wave Functions for Condensed Phases of Helium*, in *Recent Progress in Many-Body Theories*, edited by C.E. Campbell and E. Krotscheck (Plenum, NY 1992).

[10] S.A. Vitiello, K.J. Runge, G.V Chester, M.H. Kalos: *Phys. Rev. B* **42**, 228 (1990).

[11] M.P. Allen, D.J. Tildesley: *Computer Simulations of liquids* (Oxford University Press, Oxford 1987). and references therein.

[12] S.A. Vitiello, K.E. Schmidt: *Phys. Rev. B* **46**, 5442 (1992).

[13] G. Jacucci, A. Rahman *Nuovo Cimento* **D4**, 341 (1984).

[14] L. Reatto: *private communication*

[15] W.G. Hoover, S.G. Gray, K.W. Johnson: *Journ. of Chem. Phys* **55**, 1128 (1971).